Available online at www.sciencedirect.com
ScienceDirect
Engineering Structures 29 (2007) 618–625
ENGINEERING STRUCTURES
www.elsevier.com/locate/engstruct

Analytical integration of cross section properties for numerical analysis of reinforced concrete, steel and composite frames

João Batista M. Sousa Jr.*, Cereno F.D.G. Muniz

Department of Civil Engineering, Escola de Minas, Universidade Federal de Ouro Preto, Brazil

Received 24 February 2006; received in revised form 3 June 2006; accepted 5 June 2006
Available online 26 July 2006

Abstract

This paper presents a procedure for numerical analysis of steel, reinforced concrete or composite cross section of arbitrary polygonal shape, based on analytical evaluation of cross section properties, i.e., section resistant forces and tangent moduli. The uniaxial stress–strain relationship is supposed to be of a piecewise polynomial type, and the subdivision of the section into subregions is performed by means of a contouring algorithm. The procedure may be easily implemented into a beam–column finite element code which works with evaluation of cross section properties at the numerical integration points.

Keywords: Composite steel–concrete columns; Cross section analysis; Reinforced concrete columns

1. Introduction

Modern structures tend to be composed of different materials in their individual elements, and in recent years innovative new construction systems have been developed and tested. Issues such as fire and earthquake resistance, ductility, durability, ease of erection and maintenance have been major concerns. Nowadays, it is common practice to have associations of reinforced and prestressed concrete, concrete-encased steel profiles and concrete filled tubes assembled together in the same structure. The behaviour of these assemblages, however, is not always covered by design codes. In that sense, experimental and numerical investigations which can lead to a better understanding of structural behaviour are of paramount importance, and the Finite Element (FE) Method has been the most popular numerical tool for engineers and researchers.

Finite element-based numerical procedures for the analysis of steel, reinforced concrete or composite steel–concrete beam–columns have been developed for decades, employing either three-dimensional analyses with solid elements or simplified formulations using beam–column elements. The latter is often regarded as providing an optimized balance between precision of results and computational cost, even though some complex phenomena which require a more sophisticated formulation may not be captured precisely. Structural analyses of large assemblages of framed elements, specifically, are an example in which the difficulties of the modelling and the excessive computational cost of 3D calculations indicate the use of frame analysis. In some cases, even one-dimensional analyses with beam–column elements may be quite expensive, which justifies attempts to develop more efficient formulations.

Composite steel–concrete construction, in particular, gives rise to structural elements with complex cross section geometries by associating steel profiles with reinforced concrete. In framed structures such as buildings and bridges, the applied loads often lead to simultaneous biaxial bending and axial forces on individual members, and this should be taken into account.

The purpose of this work is to present a numerical procedure for the analysis of reinforced concrete, bare steel or composite steel–concrete cross sections, regarded either as isolated elements or as parts of a framed structure composed of beam–column elements. The procedure relies on a simple description of cross section geometry and uniaxial stress–strain

* Corresponding address: Departamento de Engenharia Civil, Escola de Minas, Universidade Federal de Ouro Preto, 35400-000, Ouro Preto-MG, Brazil. Tel.: +55 31 35591564; fax: +55 31 35591548.
E-mail address: joao@em.ufop.br (J.B.M. Sousa Jr.).

0141-0296/$ - see front matter © 2006 Elsevier Ltd. All rights reserved.
doi:10.1016/j.engstruct.2006.06.002

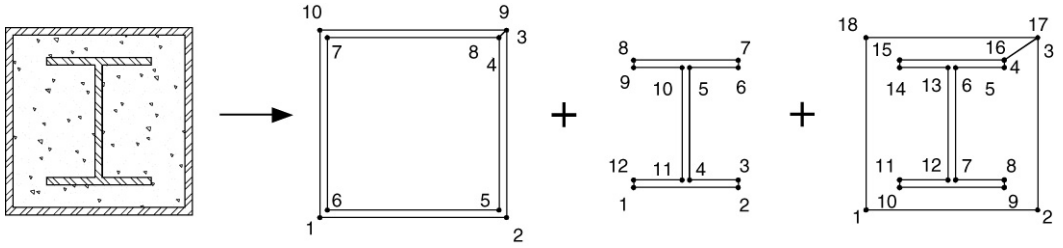

Fig. 1. Cross section material polygon definitions.

relationships of each component material, provided that some effects such as local buckling, section distortion and warping are not considered, and may be easily employed by FE programs that evaluate member behaviour by evaluation of cross section properties at their integration points. The procedure is exact, in the sense that no numerical integration is performed.

2. Cross section analysis

Cross section analysis plays a major role in the context of the one-dimensional FE analysis of steel, reinforced concrete and composite columns. Numerical and analytical procedures for the evaluation of cross section properties and responses have been developed for several decades and this is still a field of intense research [1–10]. Moreover, it is fundamental for local analyses, such as determination of strength envelopes in terms of resultant forces, or local critical section verifications which are prescribed by some widely used design codes [4,17].

According to Izzuddin [15], the two main issues related to one-dimensional element implementation are (i) determination of cross section response and (ii) integration of this response over the element length to obtain responses in terms of element degrees of freedom. In the present paper the focus is on the first issue, in a way that can be applied to a generic multi-material cross section and to structures made of reinforced concrete, steel composite or any other material association provided that some basic assumptions apply.

2.1. Basic assumptions

The cross section geometry is defined by a number of closed polygonal loops, each one with its own material. External boundaries are described clockwise and holes are described anti-clockwise (Fig. 1). Reinforcement bars are considered to be small enough to be represented by a point inside of the concrete polygon.

Assuming that cross sections remain plane after deformation (and a perfect bond between the materials), and that the bar lies along the z axis, the state of a cross section in the x–y plane may be given in terms of generalized deformation variables

$$\epsilon_z = \epsilon_0 + \kappa_x y - \kappa_y x \tag{1}$$

where ϵ_0 is the axial strain at the element reference axis, and κ_x and κ_y are the curvatures about their respective axes. These generalized deformation variables are obtained from element displacement derivatives in the most usual (displacement-based) FE formulations. Some flexibility-based or mixed formulations, on the other hand, require local state evaluations to obtain these generalized strains. Other formulations employ interpolation of the generalized variables themselves.

The cross section reference axis need not be located at any particular point, although it has been noted that under biaxial bending conditions the plastic centroid of the cross section provides better convergence properties [3].

Other variables may be used to represent the section state. Alternatively, one could employ one single curvature value κ_0, plastic centroid strain ϵ_0 and angular position of the neutral axis α, defining auxiliary (rotated) axes. This description has the advantage of allowing the representation of the geometric variation of ϵ with a single coordinate, for a fixed orientation of the neutral axis:

$$\epsilon = \epsilon_0 + \kappa\eta. \tag{2}$$

As the position of the rotated axes is a function of α the transformation between the systems involves a careful treatment of eventual singularities.

The section resultant forces are defined by

$$N_{Rz} = \int \sigma_z \, \mathrm{d}A \tag{3}$$

$$M_{Rx} = \int \sigma_z y \, \mathrm{d}A \tag{4}$$

$$M_{Ry} = -\int \sigma_z x \, \mathrm{d}A. \tag{5}$$

The tangent sectional material moduli (also called section stiffness matrix) are the derivatives of the forces with respect to the generalized deformation variables:

$$\mathbf{k_S} = \begin{bmatrix} \dfrac{\partial N_{Rz}}{\partial \epsilon_0} & \dfrac{\partial N_{Rz}}{\partial \kappa_x} & \dfrac{\partial N_{Rz}}{\partial \kappa_y} \\ \dfrac{\partial M_{Rx}}{\partial \epsilon_0} & \dfrac{\partial M_{Rx}}{\partial \kappa_x} & \dfrac{\partial M_{Rx}}{\partial \kappa_y} \\ \dfrac{\partial M_{Ry}}{\partial \epsilon_0} & \dfrac{\partial M_{Ry}}{\partial \kappa_x} & \dfrac{\partial M_{Ry}}{\partial \kappa_y} \end{bmatrix}. \tag{6}$$

The elements from the first line of (6) may be obtained from

$$\frac{\partial N_{Rz}}{\partial \epsilon_0} = \int \frac{\partial \sigma_z}{\partial \epsilon_0} \mathrm{d}A = \int \frac{\partial \sigma_z}{\partial \epsilon} \frac{\partial \epsilon}{\partial \epsilon_0} \mathrm{d}A = \int E_T \, \mathrm{d}A \tag{7}$$

$$\frac{\partial N_{Rz}}{\partial \kappa_x} = \int \frac{\sigma_z}{\partial \kappa_x} \mathrm{d}A = \int \frac{\partial \sigma_z}{\partial \epsilon} \frac{\partial \epsilon}{\partial \kappa_x} \mathrm{d}A = \int E_T y \mathrm{d}A \tag{8}$$

$$\frac{\partial N_{Rz}}{\partial \kappa_y} = \int \frac{\partial \sigma_z}{\partial \kappa_y} \mathrm{d}A = \int \frac{\partial \sigma_z}{\partial \epsilon} \frac{\partial \epsilon}{\partial \kappa_y} \mathrm{d}A = -\int E_T x \mathrm{d}A. \quad (9)$$

Similar equations arise from the derivation of M_{Rx} and M_{Ry} with respect to the generalized deformation variables. The last terms of the previous expressions are commonly used in the development of frame FE formulations.

It should be noted that in the previous expressions the terms corresponding to the presence of reinforcement were omitted. The reason is that there is no need to perform area integration as each bar is assumed to be degenerated to a point, so that the implementation of resistant forces and tangent stiffnesses is direct.

Every integral from the previous expressions (Eqs. (3)–(9)) may be divided into a simple sum of integral expressions over its various constituent materials. For the sake of conciseness, however, subsequent integral expressions will be displayed for isolated material polygons.

The central problem of cross section analysis is the evaluation of (3)–(5) and (6) and may be performed in many different ways. Roughly speaking, they may be divided into *numerical* and *analytical* procedures.

Among the numerical procedures, in the case of biaxial bending the *fiber method* is the most popular. The cross section is subdivided in a number of fibers over which the axial strain is assumed constant, and simple summations evaluate an approximation to the integral expressions by the midpoint rule. For in-plane bending the subdivision may be in layers parallel to the neutral axis. The advantages of this method are clear: it can be very easily implemented into an existing FE code, can be applied to generic cross sections and may be used in situations where strain reversal occurs (the incremental state variables are then stored for each fiber). Its main drawbacks are the computational cost and the difficulties inherent to the discretization of a generic cross section into fibers.

Several academic and commercial codes successfully employ the fiber method. For instance, Kim and Lee [18] applied the fiber model to RC columns and El-Tawil and Deierlein [13,14] to composite frames, among many others.

Other numerical integration schemes are possible such as trapezoidal, Simpson, Gauss or Lobatto rules. A study on the suitability of these integration schemes was carried out by Saje et al. [16]. However, complex geometries and biaxial bending pose difficulties on numerical integration as the integration domains become irregular polygons.

To overcome this geometrical problem, alternative procedures have been developed, and some involved numerical integration along the cross section boundaries after some transformation by Green's theorem. Others provided practical ad hoc solutions for the most common section geometries, but a generic procedure applicable to unusual cross sections seems not to have been presented yet.

These analytical integration strategies, unlike the fiber integration method, have the disadvantage of not being able to track the evolution of the state variables. Therefore they are mostly used for structures subjected to monotonic loading, unless a resultant force plasticity model is employed [13].

A family of suitable analytical procedures employs Green's theorem to transform the area integrals on boundary line integrals, in order to obtain analytically integrable functions and closed-form expressions which can be readily coded. These techniques are exact, reliable and fast. Among these, the early works of Werner [19] and Rotter [20] may be cited.

In the present work, a cross section formulation which deals with arbitrary polygonal geometries is sought. It is assumed that the uniaxial stress–strain relationship of each material is composed of a set of polynomial expressions which are piecewise continuous, which is the common case for concrete and also steel. Although the procedure may be easily employed to increasing polynomial degrees the highest order developed here is the cubic expression

$$\sigma(\epsilon) = a + b\epsilon + c\epsilon^2 + d\epsilon^3. \quad (10)$$

This consideration allows the inclusion of several well-employed uniaxial constitutive relations for concrete, steel and reinforcement, as well as the construction of close approximations to more complicated laws.

From Eqs. (3) to (5) it may be seen that the resultant forces are polynomials in ϵ and, by virtue of (1), are polynomials on x and y. The derivatives of the deformation variables with respect to the axial strain ϵ are either constant or linear on x and y. The expression $\partial\sigma_z/\partial\epsilon$ is a polynomial expression in ϵ, and therefore also on x and y. From these considerations, every term of the resultant stress field or tangent material moduli may be written in the form

$$\int_A x^m y^n \, \mathrm{d}A. \quad (11)$$

Recalling the expression for Green's theorem, where P and Q are smooth functions of (x, y), one has

$$\int\int_A \left(\frac{\partial Q}{\partial x} - \frac{\partial P}{\partial y}\right) \mathrm{d}A = \oint_{\partial A} (P\mathrm{d}x + Q\mathrm{d}y), \quad (12)$$

and over a closed domain A, by simple inspection and setting $P(x, y) = 0$, one may find a possible transformation between the integral expression (11) and the line integral over its boundary ∂A

$$\int_A x^m y^n \, \mathrm{d}A = \int_{\partial A} \frac{1}{m+1} x^{m+1} y^n \mathrm{d}y. \quad (13)$$

Assuming that the boundaries of the cross section elements are composed of straight segments, each segment from (x_i, y_i) to (x_{i+1}, y_{i+1}) may be parameterized in terms of a single variable s

$$x(s) = x_i + s(x_{i+1} - x_i) \qquad y(s) = y_i + s(y_{i+1} - y_i) \quad (14)$$

with $s = 0 \ldots 1$. The integrand in (13) is then a polynomial on s, $\mathrm{d}y = \mathrm{d}s(y_{i+1} - y_i)$ holds, and closed form expressions for the line integrals may be easily obtained for any value of m and n. Some of these expressions are presented in the Appendix.

Knowing how to integrate the sectional properties over a polygon for a generic cubic stress–strain relation, one needs to isolate, for each section material, the areas corresponding to

individual subranges of its constitutive law. This will generate a number of subpolygons inside the same material, each one corresponding to a different expression in the stress–strain relation $\sigma = \sigma(\epsilon)$.

2.2. Definition of subpolygons

With piecewise defined stress–strain relationships, it is necessary to determine, for each material, the regions over which each individual polynomial expression is valid.

With the strains at a generic point evaluated by a linear expression in x and y, one may obtain these subregions using a surface contouring algorithm [12] originally developed to display isovalues of meshes in FE analyses. The steps to obtain the individual polygons may be summarized as follows:

- for each material in the cross section
  - assemble a table to store a list of vertices for each subrange of the complete stress–strain relation.
  - For each line segment of the polygon:
    - classify the initial vertex with respect to a subrange, and store it at the corresponding subrange table entry. Also store it for processing the last edge (as it will be the final vertex).
    - Find internal points corresponding to a change of subranges; if these points exist, store them in both subranges' table entries, until the final vertex is stored. A recursive subroutine may be used to treat each segment.
  - At the end of the process a list of points which defines each subregion is defined.

This procedure is illustrated in Fig. 2 for a single material cross section with 9 vertices and 3 subranges of stress–strain relationship $\sigma_1(\epsilon)$, $\sigma_2(\epsilon)$ and $\sigma_3(\epsilon)$, each one valid for fixed strain limits. A possible section deformation is shown, as well as the angle α which may be defined as

$$\tan\alpha = \frac{\kappa_y}{\kappa_x}. \tag{15}$$

In Fig. 2, ϵ_i^n and ϵ_f^n represent the initial and final strains for subrange n. The process starts with vertex 1, whose strain ϵ is in the first range. Checking out edge 1–2, one finds out that vertex 2 is in the second range. So there was a change of ranges and it is a simple operation to find the point(s) where this happened (the edge could even have jumped across more limit strain values). From Fig. 2, let a be this point. After processing the first edge, vertex 1 would be in the row corresponding to σ_1, and point a would be inserted into both rows σ_1 and σ_2. Repeating the operation for the 9 edges, the final table contains the vertices of the subpolygons for each stress–strain relation. Table 1 shows the result of the algorithm for this case, and Fig. 3 displays the resulting polygons.

Depending on the state of strains one or more of the stress–strain relations may not be present. Generic polygonal cross sections may be employed. The algorithm works in the case of nonconvex and multiply connected domains, and repeated segments may be filtered out before the integral evaluations to save computer time.

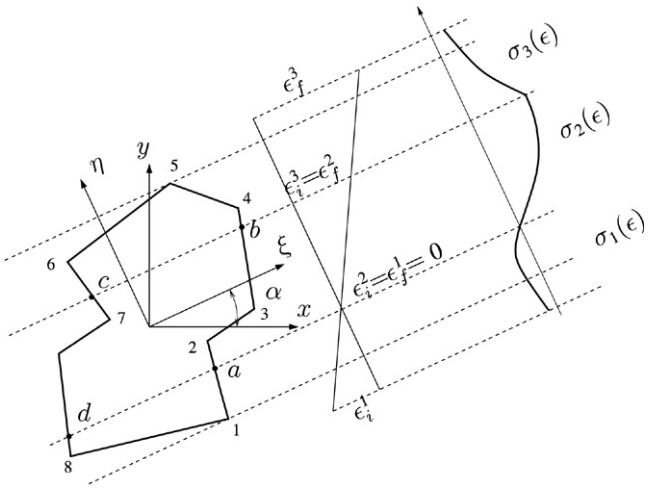

Fig. 2. Subdivision of a single material cross section with 3 subranges.

Table 1
Results for polygon subdivision

$\sigma_1 \rightarrow$	1	*a*	*d*	8			
$\sigma_2 \rightarrow$	*a*	2	3	*b*	*c*	7	*d*
$\sigma_3 \rightarrow$	*b*	4	5	6	*c*		

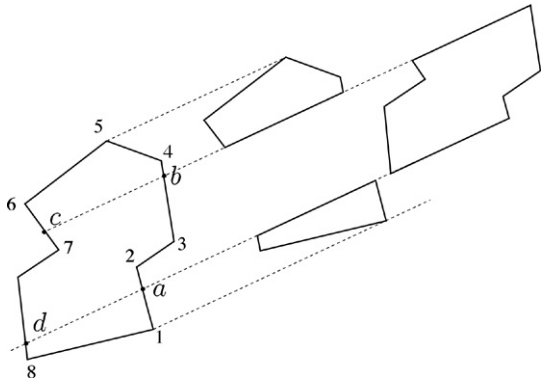

Fig. 3. Individual polygons resulting for each stress–strain relation.

Sousa Jr. and Caldas [11] employed a similar technique to analyze composite columns, restricted to specific cross sections such as concrete-encased steel profiles and concrete-filled tubes.

It may be noted that some frequently used uniaxial stress–strain relations for concrete are not expressed in terms of polynomials. These equations are rational polynomials and their analytical treatment by procedures similar to the aforementioned poses some difficulty. Recently, Zupan and Saje [10] proposed a method of analytical integration which by means of a clever change of variables permits the exact evaluation of a concrete stress–strain relationship of a rational type.

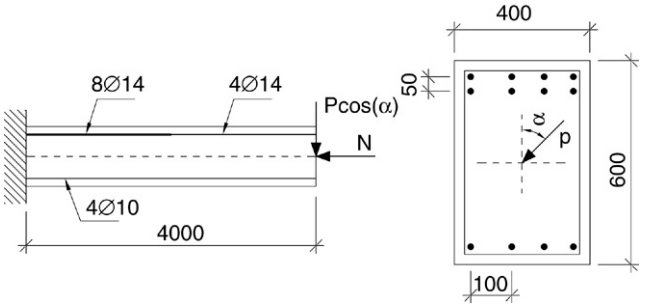

Fig. 4. Cantilever RC beam with varying reinforcement.

3. Finite element analysis

The cross section procedures presented before may be employed in any FE formulation that works with numerical integration of element properties at the section level. Two different formulations have been implemented employing the cross section procedures described in the previous section: a displacement based lagrangian formulation and a corotational formulation.

The displacement-based formulation employs cubic transverse displacement interpolation and quadratic interpolation for the axial displacement, see [11] for details.

The corotational formulation is essentially the one presented, for instance, in the book by Crisfield [21] with properly adjusted matrices to account for material nonlinearity.

4. Numerical examples

This section presents some results obtained with the cross section analysis presented in the previous sections. Examples of reinforced concrete, composite and bare steel framed structures are presented to illustrate the applicability of the formulation.

4.1. Izzuddin et al. [15] reinforced concrete beam–column

Izzuddin and coworkers [15] developed a numerical method for the analysis of RC beam–columns under axial load and biaxial bending. They analyzed a cantilever rectangular column with variable reinforcement along the column length and also unsymmetrically positioned bars in the cross section, Fig. 4. The applied normal force N is taken as 0, 500 and 1000 kN, and the transverse load P is inclined of α with respect to the cross section vertical line. Concrete resistance f_c is 20 N/mm^2, and its stress–strain is a parabola with peak f_c at the strain $\epsilon_0 = 0.002$. Reinforcement is taken as linear elastic with modulus $E = 200\ 000$ N/mm^2. The original paper presented results for cubic (10 elements) and quartic (1 single element) which are compared with the formulation presented in this paper, with four displacement-based cubic elements. Fig. 5 shows the comparative results for the three levels of normal force and for $\alpha = 0°$. Fig. 6 shows the same results for $\alpha = 90°$, and Fig. 7 shows the cantilever response for several intermediate values of α in terms of transverse displacements and for $N = 500$ kN. It may be seen that the results display a very good agreement.

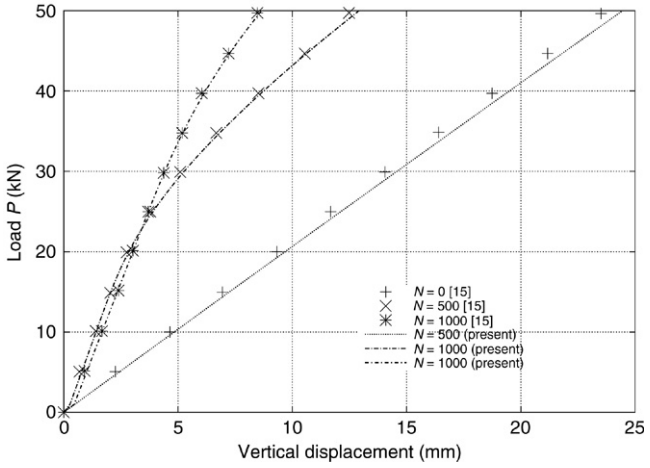

Fig. 5. Cantilever beam displacements for $\alpha = 0°$.

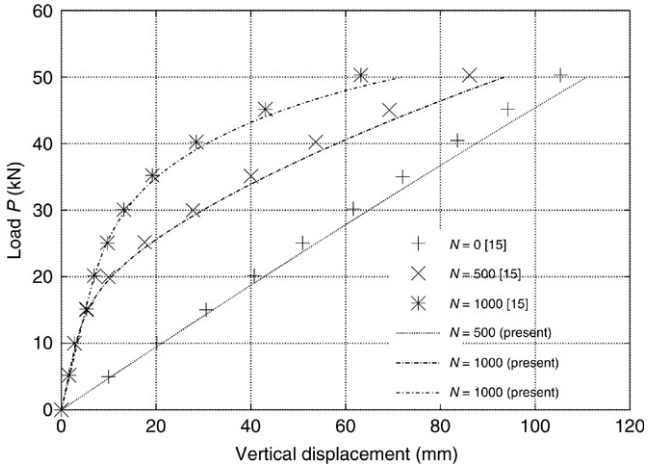

Fig. 6. Cantilever beam displacements for $\alpha = 90°$.

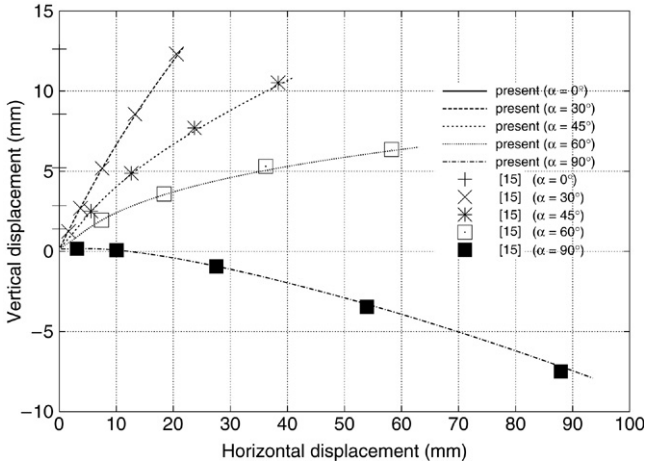

Fig. 7. Cantilever beam displacements for variable α ($N = 500$).

4.2. Han et al. [9] double skin composite columns

Han and coworkers [9] performed an experimental investigation on composite double skin beam–columns (circular

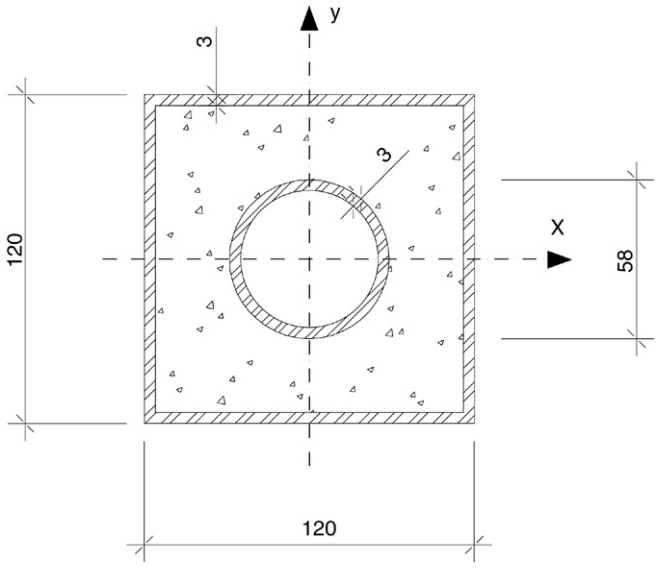

Fig. 8. Double skin cross section.

Table 2
Results for double skin columns (adapted from [9])

Specimen	Length (mm)	e (mm)	Test (t)	Numeric (n)	n/t
1a	1070	4	856	846	0.99
1b	1070	4	872	847	0.97
2a	1070	14	667	692	1.04
2b	1070	14	750	692	0.92
3a	1070	45	480	432	0.90
3b	1070	45	486	432	0.89
4a	2136	0	920	805	0.88
4b	2136	0	868	805	0.93
5a	2136	15.5	596	564	0.95
5b	2136	15.5	570	564	0.99
6a	2136	45	380	359	0.94
6b	2136	45	379	359	0.95

hollow inner and square hollow outer) filled with concrete between the steel sections (Fig. 8) and proposed a simplified analytical procedure for the evaluation of the resistance of these types of columns. The square external tube had 120 mm outer side and the circular inner tube had 58 mm external diameter, both with 3 mm plate thickness. The average concrete cubic resistance was 46.8 MPa, and the steel had 200 000 MPa elastic modulus. The external and internal tubes had yield strengths of 275.9 MPa and 374.5 MPa respectively. These cross section geometries are not covered by the most used design codes, therefore numerical and experimental analyses are of great importance for the understanding of their behaviour.

Six different pairs of columns were tested with different lengths. The results for the limit load are presented in Table 2, where e is the eccentricity of the applied load (single curvature bending).

Four corotational elements with two integration points were employed in this example. The circular hollow section was

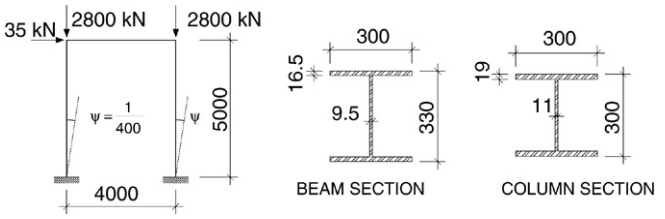

Fig. 9. Vogel steel frame (dimensions in mm).

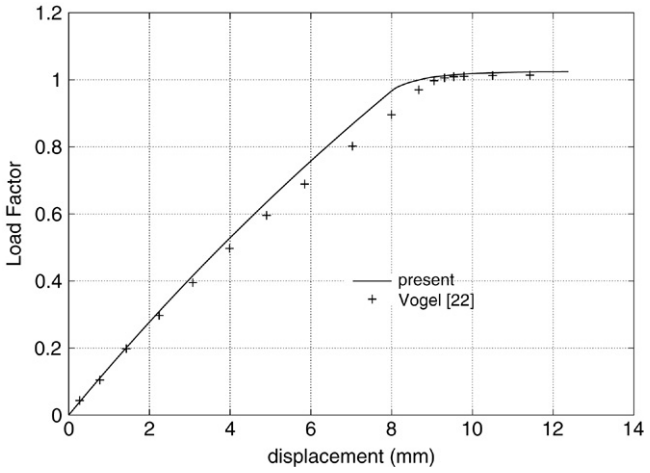

Fig. 10. Displacement results for Vogel steel frame.

modeled with straight segments connecting boundary points at every 10 degrees, with a total number of 36 segments.

4.3. Vogel frame

To illustrate the possibility of consideration of bare steel structural elements the Vogel frame [22] was modeled in this example with four corotational elements per member with two integration points in each element (Fig. 9). The figure illustrates the geometry of the frame which has an initial imperfection (out-of-straightness). The material has an elastic modulus of 205 000 MPa and yield stress of 235 MPa. Fig. 10 shows the displacements versus the load factor which multiplies all the applied loads. Once again there is good agreement between the results and the numerical values obtained by Vogel [22].

5. Summary and conclusions

The present work presented a unified methodology for the sectional (at the integration point level) numerical analysis of framed structures made of reinforced concrete, steel and composite members based on analytical integration of polynomial stress–strain material relations on arbitrary polygonal cross-sections.

The main advantage of the proposed scheme is its ability to analyze a wide range of section geometries as well as uniaxial constitutive laws. The obtained results are exact as long as the cross section segments are straight lines and the uniaxial stress–strain relations are piecewise polynomials. The main

disadvantage is the impossibility of modeling situations with strain reversal.

The procedure was coded into a general-purpose direct stiffness method program for the nonlinear analysis of some framed structures to verify its exactness and robustness and provided very good results.

Acknowledgement

The writers wish to thank V&M Tubes do Brasil for their support in the form of a grant to the second author.

Appendix A

A.1. Analytical expressions for section forces and stiffnesses

For a closed polygon with deformational state described by ϵ_0, κ_x and κ_y over which a cubic polynomial stress–strain relation must be integrated (see Eq. (10)), let

$$I_{mn} = \int x^m y^n \mathrm{d}A. \tag{A.1}$$

The normal force is given by

$$\begin{aligned} N = {} & (a + b\epsilon_0 + c\epsilon_0^2 + d\epsilon_0^3) I_{00} \\ & - \kappa_y (b + 2c\epsilon_0 + 3d\epsilon_0^2) I_{10} + \kappa_x (b + 2c\epsilon_0 + 3d\epsilon_0^2) I_{01} \\ & + \kappa_y^2 (c + 3d\epsilon_0) I_{20} - \kappa_x \kappa_y (2c + 6d\epsilon_0) I_{11} \\ & + \kappa_x^2 (c + 3d\epsilon_0) I_{02} - \kappa_y^3 d I_{30} + 3\kappa_x \kappa_y^2 d I_{21} \\ & - 3\kappa_x^2 \kappa_y d I_{12} + \kappa_x^3 d I_{03}. \end{aligned} \tag{A.2}$$

It is worth noting that for the evaluation of M_x and M_y, the expressions are very similar: to obtain M_x it is only necessary to substitute in the previous expression each I_{mn} for $I_{m,n+1}$, and to obtain M_y, just change signs of every term and change from I_{mn} for $I_{m+1,n}$. The evaluation of the external coefficients may be done only once thus saving computational time. Moreover, the expressions are developed for the complete cubic stress–strain relation, and lower degrees are simpler to evaluate.

The expressions for $\partial N/\partial \epsilon_0$, as well as $\partial N/\partial \kappa_x$ and $\partial N/\partial \kappa_y$, may be easily obtained from (A.2), after which once again a simple modification of I_{mn} (and change of signs) suffices for the evaluation of the derivatives of the moments with respect to the deformational variables. In the next section the analytical expressions for I_{mn} are presented.

A.2. Analytical expressions for I_{mn}

The following expressions are the analytical integrals of the expression $\int x^a y^b \mathrm{d}A$, after application of Green's theorem, in a line segment from (x_1, y_1) to (x_2, y_2), which is part of the closed boundary of A. Let $\Delta x = x_2 - x_1$ and $\Delta y = y_2 - y_1$. It is worth noting that because of the parametrization adopted every expression may be stated in terms of Δy, i.e. segments parallel to the x-axis do not contribute. The expressions are the ones suitable for integration of stresses and tangent moduli up to cubic stress–strain relationships. The final expression for the integrals is $I_{mn} = \sum I_{mn}^{\mathrm{S}}$

$$I_{00}^{\mathrm{S}} = \frac{\Delta y}{2}(x_1 + x_2) \tag{A.3}$$

$$I_{10}^{\mathrm{S}} = \Delta y \left(\frac{x_1^2}{2} + \frac{x_1 \Delta x}{2} + \frac{\Delta x^2}{6} \right) \tag{A.4}$$

$$I_{01}^{\mathrm{S}} = \Delta y \left(x_1 y_1 + \frac{\Delta x y_1 + \Delta y x_1}{2} + \frac{\Delta x \Delta y}{3} \right) \tag{A.5}$$

$$\begin{aligned} I_{11}^{\mathrm{S}} = {} & \frac{\Delta y}{2} \left(x_1^2 y_1 + \frac{1}{2}(x_1^2 \Delta y + 2 x_1 y_1 \Delta x) \right. \\ & \left. + \frac{1}{3}(2 x_1 \Delta x \Delta y + \Delta x^2 y_1) + \frac{1}{4} \Delta x^2 \Delta y \right) \end{aligned} \tag{A.6}$$

$$I_{20}^{\mathrm{S}} = \frac{\Delta y}{3} \left(x_1^3 + \frac{3}{2} x_1^2 \Delta x + x_1 \Delta x^2 + \frac{\Delta x^3}{4} \right) \tag{A.7}$$

$$\begin{aligned} I_{02}^{\mathrm{S}} = {} & \Delta y \left(x_1 y_1^2 + x_1 y_1 \Delta y + \frac{x_1 \Delta y^2}{3} + \frac{y_1^2 \Delta x}{2} \right. \\ & \left. + \frac{2}{3} y_1 \Delta x \Delta y + \frac{1}{4} \Delta x \Delta y^2 \right) \end{aligned} \tag{A.8}$$

$$\begin{aligned} I_{12}^{\mathrm{S}} = {} & \frac{\Delta y}{2} \left(x_1^2 y_1^2 + x_1^2 y_1 \Delta y + \frac{1}{3} x_1^2 \Delta y^2 + x_1 \Delta x y_1^2 \right. \\ & + \frac{4}{3} x_1 y_1 \Delta x \Delta y + \frac{1}{2} x_1 \Delta x \Delta y^2 + \frac{1}{3} \Delta x^2 y_1^2 \\ & \left. + \frac{1}{2} \Delta x^2 y_1 \Delta y + \frac{1}{5} \Delta x^2 \Delta y^2 \right) \end{aligned} \tag{A.9}$$

$$\begin{aligned} I_{21}^{\mathrm{S}} = {} & \frac{\Delta y}{3} \left(x_1^3 y_1 + \frac{3}{2} x_1^2 y_1 \Delta x + x_1 \Delta x^2 y_1 + \frac{1}{4} \Delta x^3 y_1 \right. \\ & \left. \frac{1}{2} x_1^3 \Delta y + x_1^2 \Delta x \Delta y + \frac{3}{4} x_1 \Delta x^2 \Delta y + \frac{1}{5} \Delta x^3 \Delta y \right) \end{aligned} \tag{A.10}$$

$$\begin{aligned} I_{22}^{\mathrm{S}} = {} & \frac{\Delta y}{180} (4 y_1 y_2 x_2^3 + 4 x_1^3 y_1 y_2 + 6 x_1 x_2^2 y_2^2 + 3 x_1^2 x_2 y_2^2 \\ & + 3 x_1 x_2^2 y_1^2 + x_1^3 y_2^2 + 10 x_2^3 y_2^2 + x_2^3 y_1^2 + 6 x_2 x_1^2 y_1^2 \\ & + 10 x_1^3 y_1^2 + 6 x_2 x_1^2 y_1 y_2 + 6 x_1 x_2^2 y_1 y_2) \end{aligned} \tag{A.11}$$

$$I_{30}^{\mathrm{S}} = \frac{\Delta y}{4} \left(x_1^4 + 2 x_1^3 \Delta x + 2 x_1^2 \Delta x^2 + x_1 \Delta x^3 + \frac{1}{5} \Delta x^4 \right) \tag{A.12}$$

$$\begin{aligned} I_{03}^{\mathrm{S}} = {} & \Delta y \left(x_1 y_1^3 + \frac{3}{2} x_1 y_1^2 \Delta y + x_1 y_1 \Delta y^2 + \frac{1}{4} x_1 \Delta y^3 \right. \\ & \left. + \frac{1}{2} \Delta x y_1^3 + y_1^2 \Delta x \Delta y + \frac{3}{4} y_1 \Delta x \Delta y^2 + \frac{1}{5} \Delta x \Delta y^3 \right) \end{aligned} \tag{A.13}$$

$$\begin{aligned} I_{13}^{\mathrm{S}} = {} & \frac{\Delta y}{120} (4 x_1 x_2 y_2^3 + x_1^2 y_2^3 + 10 x_2^2 y_2^3 + 6 x_1 x_2 y_1 y_2^2 \\ & + 3 y_1 x_1^2 y_2^2 + 6 y_1 x_2^2 y_2^2 + 3 x_2^2 y_1^2 y_2 + 6 x_1 x_2 y_1^2 y_2 \\ & + 4 x_1 x_2 y_1^3 + 10 x_1^2 y_1^3 + x_2^2 y_1^3 + 6 x_1^2 y_1^2 y_2) \end{aligned} \tag{A.14}$$

$$\begin{aligned} I_{31}^{\mathrm{S}} = {} & \frac{\Delta y}{120} (2 x_2 y_2 x_1^3 + 5 x_1^4 y_1 + 2 x_1 x_2^3 y_1 + 3 x_1^2 x_2^2 y_2 \\ & + 3 x_1^2 x_2^2 y_1 + 4 x_1^3 x_2 y_1 + 5 x_2^4 y_2 + x_2^4 y_1 + x_1^4 y_2 \\ & + 4 x_1 x_2^3 y_2) \end{aligned} \tag{A.15}$$

$$I_{04}^{S} = \frac{\Delta y}{30}(5x_2y_2^4 + x_2y_1^4 + 3x_1y_1^2y_2^2 + 2x_2y_1^3y_2 + 3x_2y_1^2y_2^2 + 4x_2y_1y_2^3 + 4x_1y_1^3y_2 + 2x_1y_1y_2^3 + 5x_1y_1^4 + x_1y_2^4) \quad (A.16)$$

$$I_{40}^{S} = \frac{\Delta y}{30}(x_1 + x_2)(x_1^2 - x_1x_2 + x_2^2)(x_1^2 + x_1x_2 + x_2^2). \quad (A.17)$$

References

[1] Rodriguez JA, Aristizabal-Ochoa JD. Biaxial interaction diagrams for short RC columns of any cross-section. Journal of Structural Engineering 1999;125(6):672–83.

[2] Sfakianakis MG. Biaxial bending with axial force of reinforced, composite and repaired concrete sections of arbitrary shape by fiber model and computer graphics. Advances in Engineering Software 1999;(33): 227–42.

[3] Chen SF, Teng JG, Chan SL. Design of biaxially loaded short composite columns of arbitrary section. Journal of Structural Engineering 2001; 127(66):678–85.

[4] Fafitis A. Interaction surfaces of reinforced concrete sections in biaxial bending. Journal of Structural Engineering 2001;127(7):840–6.

[5] Bonet JL, Romero ML, Miguel PF, Fernandez MA. A fast stress integration algorithm for reinforced concrete sections with axial loads and biaxial bending. Computers & Structures 2004;82(2–3):213–25.

[6] Bonet JL, Miguel PF, Fernandez MA, Romero ML. Analytical approach to failure surfaces in reinforced concrete sections subjected to axial load and biaxial bending. Journal of Structural Engineering 2004;130(12): 2006–15.

[7] Pisani MA. A numerical method to analyze compact cross-sections. Computers & Structures 1996;59(6):1063–72.

[8] Pisani MA. Non-linear strain distributions due to temperature effects in compact cross-sections. Engineering Structures 2004;26(10):1349–63.

[9] Han LH, Tao Z, Huang H, Zhao XL. Concrete-filled double skin (SHS outer and CHS inner) steel tubular beam–columns. Thin-Walled Structures 2004;42(9):1329–55.

[10] Zupan D, Saje M. Analytical integration of stress field and tangent material moduli over concrete cross-sections. Computers & Structures 2005;(83):2368–80.

[11] Sousa Jr JBM, Caldas RB. Numerical analysis of composite steel–concrete columns of arbitrary cross section. Journal of Structural Engineering 2005;131(11):1721–30.

[12] Martha LF, Carvalho MTM, Seixas RB. Volume contouring of generic unstructured meshes. Journal of the Brazilian Computer Society 1997; 3(3):43–51.

[13] El-Tawil S, Deierlein GG. Nonlinear analysis of mixed steel–concrete frames. I: Element formulation. Journal of Structural Engineering 2001; 127(6):647–55.

[14] El-Tawil S, Deierlein GG. Nonlinear analysis of mixed steel–concrete frames. II: Implementation and verification. Journal of Structural Engineering 2001;127(6):656–65.

[15] Izzuddin BA, Siyam AAFM, Lloyd Smith D. An efficient beam–column formulation for 3D reinforced concrete frames. Computers & Structures 2001;80:659–76.

[16] Saje M, Planinc I, Turk G, Vratanar B. A kinematically exact finite element formulation of planar elastic–plastic frames. Computer Methods in Applied Mechanics and Engineering 1997;144:125–51.

[17] Bonet JL, Miguel PF, Fernandez MA, Romero ML. Biaxial bending moment magnifier method. Engineering Structures 2004;26(13):2007–19.

[18] Kim JK, Lee SS. The behavior of reinforced concrete columns subjected to axial force and biaxial bending. Engineering Structures 2000;22(10): 1518–28.

[19] Werner H. Schiefe Biegung polygonal umrandeter Stahlbeton-Querschnitte. Beton-und Stahlbetonbau 1974;69(4):92–7.

[20] Rotter JM. Rapid exact inelastic biaxial bending analysis. Journal of the Structural Division – ASCE 1985;111:2659–74.

[21] Crisfield MA. Nonlinear finite element analysis of solids and structures, vol. 1. Essentials. Wiley; 1991.

[22] Vogel U. Calibrating frames. Stahlbau 1985;10:295–301.